From Inelastic Neutron Scattering to Structural Information. A Two-Dimensional Parametrized Model To Study Metal−(H_2) Interaction

Eric Clot*,† and Juergen Eckert‡

Contribution from LSDSMS (UMR 5636) CC 014, Université de Montpellier II, 34095 Montpellier cedex 05, France, and LANSCE MS H805, Los Alamos National Laboratory, Los Alamos, New Mexico 87545

Received October 14, 1998. Revised Manuscript Received June 17, 1999

Abstract: A two-dimensional dynamical parametrized model is derived to study the M−(H_2) interaction in transition-metal molecular hydrogen complexes. The parameters have been adjusted to reproduce the observed inelastic neutron scattering transitions through a least-squares fit procedure. The vibrational levels are obtained by solving the nuclear Schrödinger equation in a discrete variable representation. From this procedure, structural information such as the barrier to rotation of the H_2 ligand and the H−H distance have been obtained. The accuracy of the model is tested on four systems with M−(H_2) interactions of different nature. The resulting H−H bond distances are in very good agreement with neutron diffraction structures where available.

Introduction

The synthesis by Kubas and co-workers[1] of the molecular hydrogen complex W(η^2-H_2)(P^iPr_3)$_2$(CO)$_3$ is certainly one of the most important discoveries in coordination chemistry during the last 15 years. Since then it has been possible to design complexes containing the H_2 ligand, namely a dihydrogen molecule H_2 bound in an η^2 mode to a transition-metal center, and still retain some bonding interaction between the two H atoms.[2−5] Moreover, some previously known "classical" polyhydrides have since been reformulated as "nonclassical" molecular hydrogen complexes.

A key property of all these complexes is the distance between the hydrogen nuclei in the H_2 ligand, which can be considerably longer (0.78−1.2 Å) than for free H_2 (0.74 Å). The elongation is a consequence of the nature of the bonding between H_2 and the metal center. The dihydrogen ligand acts as a σ donor through its occupied σ molecular orbital (σ donation) and as a π acceptor through its unoccupied σ^* MO (π back-donation). Both effects contribute to weaken the H−H bond and eventually break it, particularly if the back-donation is strong. This results in a classical dihydride, which was the only class of compounds known before 1984. However, the σ Lewis acidity and π Lewis basicity of the metal fragment L_nM can be modified by appropriate ligand design, and the synergy between the two aforementioned electronic interactions may then yield a nonclassical structure. Since the problem of bond activation is of fundamental importance in homogeneous catalysis, it is essential to obtain an improved understanding of the interaction between H_2 and a metal center, which in turn can be provided by studies of molecular hydrogen complexes.

Unfortunately the determination of the H−H distance, perhaps the most important experimental measure of bond activation, in M−(η^2-H_2) compounds is a very difficult experimental problem. This is best done by neutron diffraction of the complex since hydrogen nuclei can be located with this technique. However, only a few neutron structures of dihydrogen complexes have been published to date[6−15] because relatively large single crystals are required. Solid-state NMR has also proven to be a very valuable tool for the determination of precise H−H bond distances.[16]

NMR spectroscopy has been used in solution in conjunction with isotopic substitution. The coupling constant J(H,D) for M−(η^2-HD) is found to be smaller than that for free HD (43.2 Hz),[17] and typical values range from 25 to 35 Hz. The decrease is the result of the elongation of the H−D bond (r_{HD}) upon

* To whom correspondence should be addressed. E-mail: clot@lsd.univ-montp2.fr.

† Universite de Montpellier II.

‡ Los Alamos National Laboratory.

(1) Kubas, G. J.; Ryan, R. R.; Swanson, B. I.; Vergamini, P.; Wasserman, H. J. *J. Am. Chem. Soc.* **1984**, *106*, 451.

(2) Kubas, G. J. *Acc. Chem. Res.* **1988**, *21*, 120.

(3) Crabtree, R. H. *Acc. Chem. Res.* **1990**, *23*, 95.

(4) Jessop, P. G.; Morris, R. H. *Coord. Chem. Rev.* **1992**, *121*, 155.

(5) Heinekey, D. M.; Oldham, W. J., Jr. *Chem. Rev.* **1993**, *93*, 913.

(6) Vergamini, P. J.; Kubas, G. J.; Ryan, R. R.; Wasserman, H. J.; Larson, A. C. *Am. Cryst. Assoc., Ser. 2* **1983**, *11*, 23.

(7) Ricci, J. S.; Koetzle, T. F.; Bautista, M. T.; Hofstede, T. M.; Morris, R. H.; Sawyer, J. F. *J. Am. Chem. Soc.* **1989**, *111*, 8823.

(8) van der Sluys, L. S.; Eckert, J.; Eisenstein, O.; Hall, J. H.; Huffman, J. C.; Jackson, S. A.; Koetzle, T. F.; Kubas, G. J.; Vergamini, P. J.; Caulton, K. G. *J. Am. Chem. Soc.* **1990**, *112*, 4831.

(9) Albinati, A.; Bakhmutov, V. I.; Caulton, K. G.; Clot, E.; Eckert, J.; Grushin, O. E. V. V.; Hauger, B. E.; Klooster, W. T.; Koetzle, T. F.; McMullan, R. K.; O'Loughlin, T. J.; Pélissier, M.; Ricci, J. S.; Sigalas, M. P.; Vymenits, A. B. *J. Am. Chem. Soc.* **1993**, *115*, 7300.

(10) Kubas, G. J.; Burns, C. J.; Eckert, J.; Johnson, S. W.; Larson, A. C.; Vergamini, P. J.; Unkefer, C. J.; Khalsa, G. R. K.; Jackson, S. A.; Eisenstein, O. *J. Am. Chem. Soc.* **1993**, *115*, 569.

(11) Klooster, W. T.; Koetzle, T. F.; Jia, G.; Fong, T. P.; Morris, R. H.; Albinati, A. *J. Am. Chem. Soc.* **1994**, *116*, 7677.

(12) Hasegawa, T.; Li, Z.; Parkin, S.; Hope, H.; McMullan, R. K.; Koetzle, T. F.; Taube, H. *J. Am. Chem. Soc.* **1994**, *116*, 4352.

(13) Eckert, J.; Jensen, C. M.; Koetzle, T. F.; Husebo, T. L.; Nicol, J.; Wu, P. *J. Am. Chem. Soc.* **1995**, *117*, 7271.

(14) Maltby, P. A.; Schlaf, M.; Steinbeck, M.; Lough, A. J.; Morris, R. H.; Klooster, W. T.; Koetzle, T. F.; Srivastava, R. C. *J. Am. Chem. Soc.* **1996**, *118*, 5396.

(15) Gross, C. L.; Young, D. M.; Schultz, A. J.; Girolami, G. S. *J. Chem. Soc., Dalton Trans.* **1997**, 3081.

(16) Zilm, K. W.; Millar, J. M. *Adv. Magn. Opt. Res.* **1990**, *15*, 163.

10.1021/ja9836141 CCC: $18.00
Published on Web 09/15/1999

coordination, and linear relationships between J(H,D) and r_{HD} have been derived from experimental data.[14,18] However, the results depend critically on which data (neutron, solid-state NMR) are used to anchor the correlation.[18] Moreover, when hydride ligands are present, rapid site exchange between the dihydrogen and the hydrides leads to the observation of a dynamically averaged value for J(H,D).[19]

The most commonly used means to determine H−H bond distances have been relaxation time measurements.[20] Because of the close proximity of the two nuclei within the H_2 ligand, the relaxation through the dipole−dipole interaction is fast and the relaxation time T_1 as a function of temperature exhibits a minimum ($T_{1,min}$) whose position depends on the strength of the magnetic field. A low value for $T_{1,min}$ (e.g., ≤80 ms) is generally considered to be an indication of the presence of an H_2 ligand in the molecule, and the H−H bond distance can then be derived.[3] However, relaxation can also be achieved by dipole−dipole interactions with other nuclei (P, Re, ...).[21] Halpern and co-workers[22] have critically studied this so-called "T_1 criterion" and found that some short $T_{1,min}$ values may be obtained without an H_2 ligand in the molecule. Moreover the value for r_{HH} deduced from T_1 measurements depends also on an assumption of the relative rate of rotation for the H_2 ligand (fast or slow).[12] T_1 experiments are thus very valuable for establishing the presence of an H_2 ligand in a given complex, but are not sufficiently unambiguous to yield accurate H−H bond distances.

Inelastic neutron scattering (INS) is another spectroscopic means for probing the existence of dihydrogen complexes. Our aim in this paper is to describe how INS can, in conjunction with a parametrized dynamical model, be used to extract precise structural information from the observed transitions, principally those related to the rotation of the H_2 ligand (*vide infra*). Eckert has been using a one-dimensional model[23] to derive a value of the barrier to rotation from the INS spectra of dihydrogen complexes. In this model the H_2 ligand is viewed as a planar rigid rotor whose equilibrium bond distance is *assumed* on the basis of other experimental or theoretical information. The model we present in this paper is a refinement of the previous one which *explicitly includes* the H−H distance in the parametrization of the dynamics. The H_2 ligand is now considered to be a nonrigid planar rotor whose Hamiltonian is parametrized. The parameters (*vide infra*) are optimized by means of a least-squares fit of the difference between the experimental and the computed values for the INS transitions. This optimization of the parameters yields very valuable structural information about the complex. In particular, the equilibrium H−H bond distances obtained from this procedure are very accurate and in excellent agreement with the experimental data where available.

Two-Dimensional Dynamical Model

Permutation of Identical Particles and INS Spectra. The H_2 molecule binds in an η^2 mode to the metal as is shown in Chart 1. The dihydrogen ligand can then adopt two extreme

Chart 1

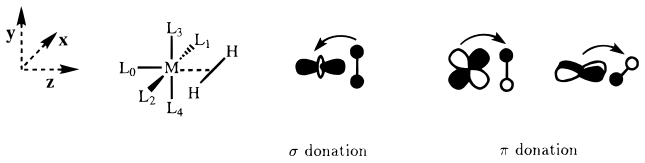

Chart 2

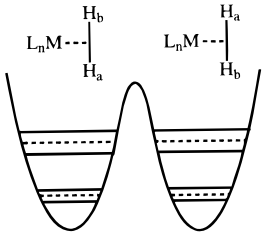

conformations, where it can be parallel to L_1-M-L_2 or parallel to L_3-M-L_4.

The preference for a particular conformation is determined by the π basic properties of the metal fragment, because σ donation from H_2 is not dependent on the orientation of the H−H axis. Stabilization through π back-donation, on the other hand, is strongly influenced by this orientation. First, the d orbitals involved (d_{yz} or d_{xz}) on the metal must be filled to accomplish some donation to H_2; second, a preferred orientation is obtained relative to the highest of the two occupied d_{yz} or d_{xz} orbitals (see Chart 1 for the definition of the axis), because this orbital is the closest in energy to the accepting $\sigma^*_{H_2}$ orbital. It is interesting to note that a large number of the known dihydrogen complexes to date have a formal d^6 electron count on the metal, as is the case for the four systems we have studied. As a consequence, both the d_{yz} and d_{xz} are filled, and therefore no particular orientation is strongly preferred. The barrier between the two conformations is therefore rather small, usually less than 3.0 kcal·mol^{-1}, which is the reason only one peak is observed for the H_2 ligand in ^{1}H NMR spectra in solution at room temperature.

Due to this low barrier the two hydrogen nuclei perform large-amplitude librational motion, which results in an interchange of their mutual positions. A qualitative potential energy profile associated with this rotation is shown in Chart 2. The process can be considered as a permutation of two identical particles in a potential created by the metal fragment L_nM, which is assumed to be frozen and thus simply constitutes a reference frame fixed in space.

The symmetry properties of the two nuclei under site exchange are described within the framework of complete nuclear permutation inversion groups,[24] namely, S_2^* for two identical particles. These groups are particularly suited for the characterization of symmetry properties in systems with large-amplitude motions where the molecular point groups are no longer a good approximation.[24,25] The particular group S_2^* consists of four operations:

$$S_2^* = \{E, E^*, (ab), (ab)^*\}$$

The E operation is the identity while the E^* operation is the inversion of all the coordinates of the H_2 molecule (electrons plus nuclei) in the center of mass. The operation (ab) corre-

(17) Bloyce, P. E.; Rest, A. J.; Whitwell, I.; Graham, W. A. G.; Holmes-Smith, R. J. *J. Chem. Soc., Chem. Commun.* **1988**, 846.
(18) Heinekey, D. M.; Luther, T. A. *Inorg. Chem.* **1998**, *37*, 127.
(19) Eckert, J.; Albinati, A.; Bucher, U. E.; Venanzi, L. M. *Inorg. Chem.* **1996**, *35*, 1292.
(20) Hamilton, D. G.; Crabtree, R. H. *J. Am. Chem. Soc.* **1988**, *110*, 4126.
(21) Cotton, F. A.; Luck, R. L.; Root, D. R.; Walton, R. A. *Inorg. Chem.* **1990**, *29*, 43.
(22) Desrosiers, P. J.; Cai, L.; Ling, Z.; Richards, R.; Halpern, J. *J. Am. Chem. Soc.* **1991**, *113*, 4173.
(23) Eckert, J. *Spectrochim. Acta* **1992**, *48A*, 363.
(24) Bunker, P. R. *Molecular Symmetry and Spectroscopy*; Academic Press: New York, 1979.
(25) Hougen, J. T. *J. Phys. Chem.* **1986**, *90*, 562.

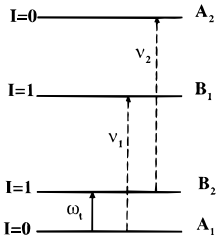

Figure 1. Qualitative energy level diagram associated with rotational tunneling in a dihydrogen complex. The observed INS transitions are shown.

sponds to the permutation of the two nuclei H_a and H_b and $(ab)^*$ is the product between E^* and (ab). S_2^* is isomorphic to C_{2v}, so the Mulliken labels A_1, A_2, B_1, and B_2 of C_{2v} are used to name the irreducible representations of S_2^*.

The symmetry under the permutation operation (ab) is crucial for the interpretation of the INS experiment. Because of the low barrier, this permutation is very easy, with the result that each of the torsional levels (dashed lines in Chart 2) is split in two (solid lines in Chart 2), which are, respectively, symmetric and antisymmetric under the exchange. Rotational tunneling can occur between two equivalent configurations, and the magnitude of this tunnel splitting is related to the height and width of the barrier to rotation. The nature of the nuclear spin wave function for each level is governed by the symmetry of the spatial wave function and the fermionic nature of hydrogen nuclei. This requires that the overall wave function for the H_2 ligand be antisymmetric under permutation of the nuclei, which gives rise to the energy level diagram shown in Figure 1 for the four lowest rotational levels.

The A_1 and A_2 (respectively, B_1 and B_2) levels are symmetric (respectively, antisymmetric) under the permutation and are associated with an antisymmetric (respectively, symmetric) nuclear spin wave function, namely, a singlet S (respectively, a triplet T) to ensure that the total wave function is antisymmetric with respect to the exchange of the two particles. A collision between the system and a beam of particles with nonzero nuclear spin (neutrons) can induce transitions between energy levels with different nuclear spins. Within the lowest level (solid line in Figure 1) it is called the rotational tunneling (ω_t) transition. Transitions to the higher lying torsional states (ν_i) can be observed (dashed lines in Figure 1) by neutron energy loss. See the review by Eckert[23] for more details.

For low frequencies the INS experiment therefore probes a tunnel effect between the two equivalent configurations of the dihydrogen ligand. This effect is very sensitive to the general shape of the potential energy surface associated with the exchange. INS is thus a highly sensitive tool for the investigation of various factors in the binding of dihydrogen in metal complexes. The nature of the metal as well as the electronic and/or steric influences of the ancillary ligands introduce small changes to the potential energy surface (PES) that are enhanced in an experiment based on a tunnel effect. This type of process (H_2 rotation in transition-metal complexes) is very difficult to simulate by *ab initio* computations. First, the size of the experimental system is too large, and therefore simplified models for the ligands (PH_3 for example as the prototype phosphine) must be used. Second, the level of the calculation cannot be of the highest quality (no optimization at the CCSD(T)[26] level) again because of the size of the complexes. As a consequence

(26) Pople, J. A.; Head-Gordon, M.; Raghavachari, K. *Chem. Phys. Lett.* **1987**, *87*, 5968.

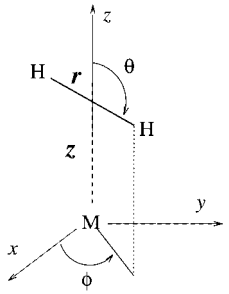

Figure 2. Definition of the dynamic coordinates involved in the exchange of the two hydrogen atoms during the rotation of the H_2 ligand.

chemical accuracy is not possible, and an error of more than 1.5 kcal·mol^{-1} on a rotation barrier lower than 3.0 kcal·mol^{-1} precludes the use of *ab initio* calculations for a quantitative description of the INS experiment. This is why at present the use of our parametrized dynamical model is a preferable alternative.

The Parametrized Hamiltonian. The system under investigation consists of two hydrogen nuclei which exchange their mutual positions in a potential created by a metal fragment. The coordinates used to locate the two hydrogen atoms with respect to the metal fragment (M) are shown in Figure 2. The center of mass G of the two nuclei is constrained to move along the z axis where $z_G = z$ is the Cartesian coordinate along this axis ($x_G = y_G = 0$). The metal fragment itself can be considered to be a fixed reference frame within which the H_2 molecule is described by the usual spherical coordinates r, θ, and ϕ (Figure 2). The complete description of the exchange process thus involves the four dynamical coordinates r, θ, ϕ, and z.

A further simplification arises from the very peculiar nature of the binding mode of H_2 to the metal. The η^2 coordination mode corresponds to $\theta = 90°$, and one can assume that, during the rotation, the H_2 ligand remains perpendicular to the z axis and is not displaced appreciably relative to the metal along z. The two coordinates z and θ do not therefore play an important role in the dynamics of the exchange in contrast to r and ϕ. The recent normal mode analysis made by Eckert et al.[27] on Kubas' compound supports this assumption as they observe higher vibrational frequencies for modes involving z and θ than those for the torsional deformation associated with ϕ. These coordinates are thus excluded from the dynamical model which now depends only on the two variables r and ϕ (2D model), where $\phi = 0$ corresponds to the reference plane which contains the metal and the H_2 ligand in the ground-state equilibrium geometry.

The H_2 ligand is then considered to be a planar rotor with a kinetic energy operator $\mathbf{T}$ and μ the reduced mass for H_2[28] (eq 1). The ϕ angle corresponds to the large-amplitude motion

$$\mathbf{T} = -\frac{\hbar^2}{2\mu r^2}\frac{\partial^2}{\partial\phi^2} - \frac{\hbar^2}{2\mu}\frac{1}{r}\frac{\partial}{\partial r}r\frac{\partial}{\partial r} \qquad (1)$$

(rotation) associated with the exchange, whereas r describes how the H_2 ligand responds to the change in ϕ. All symmetry properties are uniquely described by the ϕ angle.[24] Table 1 shows how ϕ transforms under the four operations of S_2^* and gives the characters of the four irreducible representations.

(27) Bender, B. R.; Kubas, G. J.; Jones, L. H.; Swanson, B. I.; Eckert, J.; Capps, K. B.; Hoff, C. D. *J. Am. Chem. Soc.* **1997**, *119*, 9179.

(28) The metal fragment ML_n is supposed to have an infinite mass compared to the H_2 ligand, so it is not included in the calculation of μ.

Table 1. Transformation Properties of the Coordinate ϕ under the Operations of S_2^* and Characters of the Irreducible Representations of the Group

	E ($\phi \rightarrow \phi$)	(ab) ($\phi \rightarrow \pi + \phi$)	E^* ($\phi \rightarrow -\phi$)	$(ab)^*$ ($\phi \rightarrow \pi - \phi$)
A_1	1	1	1	1
A_2	1	1	−1	−1
B_1	1	−1	−1	1
B_2	1	−1	1	−1

The two coordinates vary on two rather different time scales. The ϕ angle is a slow variable while the H−H distance r adapts itself rapidly to changes in ϕ as is indicated by the difference in vibrational frequency for the two coordinates.[27,29] An adiabatic approximation can therefore be made and the dynamics treated within the framework of the reaction path Hamiltonian of Miller.[30,31] The potential is described by separating out a reaction coordinate and assuming that the other degrees of freedom are adiabatic. More specifically, for a fixed value of ϕ, the potential is expanded in power series of r. In the case of dihydrogen complexes, the variation in r during the rotation is small, and therefore only the harmonic term is considered. The two-dimensional potential $V(r,\phi)$ is then written as in eq 2. The

$$V(r,\phi) = V(\phi) + (1/2)\mu\omega^2(\phi)\{r - r_{eq}(\phi)\}^2 \qquad (2)$$

potential along the ϕ coordinate must transform as the irreducible representation A_1 of S_2^* (Table 1), and it is therefore expanded in a set of functions that are of A_1 symmetry (eq 3).

$$V(\phi) = \sum_{n=1}^{N} V_{2n}\{1 - \cos(2n\phi)\} \qquad (3)$$

The general expression for the Hamiltonian of the 2D model is the sum of the kinetic energy operator (eq 1) and the potential energy operator (eqs 2 and 3). A parametrized Hamiltonian for the specific dynamics under study can be built in several ways. We have chosen to introduce parameters that have a clear physical meaning and that are relevant to the chemistry of the dihydrogen complexes. In addition the number of parameters must be kept small since there are few experimentally observed transitions to reproduce. We have therefore chosen *four parameters*: first, the height V_0 of the barrier to rotation is defined in eq 4 where $\phi = 0$ corresponds to the configuration

$$V_0 = V(\phi = \pi/2) - V(\phi = 0) \qquad (4)$$

of the H_2 ligand in the equilibrium geometry. For the second parameter we have chosen the width of the barrier, since for tunneling both the height and the width of the barrier are important. The width is characterized by the angle α defined in eq 5. This angle is the width of the barrier at half-height. The

$$\frac{V_0}{2} = V(\phi = \pi/2 - \alpha/2) = V(\phi = \pi/2 + \alpha/2) \qquad (5)$$

third and fourth parameters r_0 and ω_0 describe the r coordinate by its equilibrium value and associated vibrational frequency. Another simplification can be made here because the H−H distance does not vary much during the rotation when ϕ goes from 0 to π. To a good approximation then $r_{eq}(\phi)$ and $\omega(\phi)$ are independent of ϕ (eqs 6 and 7).

$$\omega(\phi) = \omega_0 \qquad (6)$$

$$r_{eq}(\phi) = r_0 \qquad (7)$$

For the potential as a function of ϕ the two conditions given by eqs 4 and 5 terminate the expansion in eq 3 at $N = 2$, where V_2 and V_4 are given in eqs 8 and 9. The final expression for

$$V_2 = V_0/2 \qquad (8)$$

$$V_4 = -\frac{V_0 \cos\alpha}{4\sin^2\alpha} \qquad (9)$$

the 2D potential is thus

$$V(r,\phi) = \frac{V_0}{2}(1 - \cos 2\phi) - \frac{V_0 \cos\alpha}{4\sin^2\alpha}(1 - \cos 4\phi) + \frac{1}{2}\mu\omega_0(r - r_0)^2 \qquad (10)$$

where V_0, α, r_0, and ω_0 are the *four parameters* of the model.

Solution of the Nuclear Schrödinger Equation. The Hamiltonian H of the 2D dynamical model involves four parameters. Solution of the nuclear Schrödinger equation for a given set of the four parameters gives the vibrational levels shown schematically in Figure 1. The energies associated with the INS transitions are then computed and compared to the experimental ones. Parameters are adjusted to improve the agreement with experiment in a least-squares sense, and the function L in eq 11 is minimized (see Figure 1 for the notation, usually $N = 2$

$$L = [w_0(\omega_t^{exp} - \omega_t^{calc})^2 + \sum_{i=1}^{N} w_i(\nu_i^{exp} - \nu_i^{calc})^2]^{1/2} \qquad (11)$$

or $N = 3$ in eq 11). The weighting factors w_0 and w_i are chosen according to the experimental accuracy of the values of the transition energies. The typical accuracy on ω_t is 0.5 cm^{-1}, while it is 5 cm^{-1} on ν_i. To take this into account in the fitting procedure, the factor w_0 is 100 times greater than the other w_i, so that an error of 0.5 cm^{-1} in ω_t would contribute to the same degree as an error of 5 cm^{-1} in ν_i.

The interested reader can find a detailed discussion of the methodology used to compute the vibrational levels in the Appendix. Most notably we demonstrate how the problem can be solved very efficiently by using a symmetry-adapted basis set built on a discrete variable representation (DVR)[32] and how this basis set has been made very compact by implementation of the sequential adiabatic reduction of Bačić and Light.[33,34]

We now illustrate the accuracy of our procedure on a particular example to be described in depth later. Four INS transitions were observed for the compound $IrClH_2(H_2)(P^iPr_3)_2$, and in Figure 3 we have plotted the variation in L when one parameter is varied and the others are held fixed at their optimal value. More specifically, it is the relative deviation (in percent) in L from the optimal value which is shown. The increments Δp for the parameters are as follows: 0.01 kcal·mol^{-1} for V_0, 1° for α, 0.005 Å for r_0, and 100 cm^{-1} for ω_0. It is obvious from Figure 3 that the three parameters V_0, α, and r_0 are very accurately computed.

Our 2D model is thus a new means to estimate H−H bond distances in molecular hydrogen complexes with very high

(29) Clot, E. Ph. D. Thesis, Université de Paris Sud, Orsay, 1995.
(30) Truhlar, D. G.; Kuppermann, A. *J. Am. Chem. Soc.* **1971**, *93*, 1840.
(31) Miller, W. H. *J. Chem. Phys.* **1980**, *72*, 99.
(32) Light, J. C.; Hamilton, I. P.; Lill, J. V. *J. Chem. Phys.* **1985**, *82*, 1400.
(33) Bačić, Z.; Light, J. C. *J. Chem. Phys.* **1986**, *86*, 3065.
(34) Light, J. C.; Bačić, Z. *J. Chem. Phys.* **1987**, *87*, 4008.

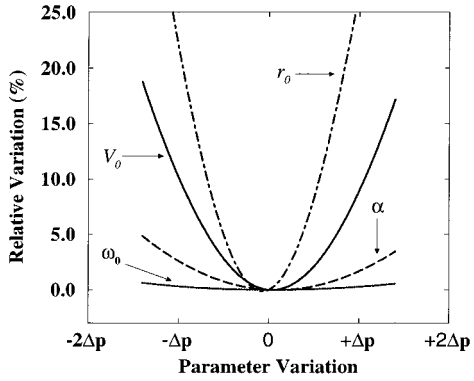

Figure 3. Relative variations (%) in L when one parameter is varied, the others being kept constant at their optimal value. $\Delta p = 0.01$ kcal·mol^{-1} for V_0, 0.005 Å for r_0, 1° for α, and 100 cm^{-1} for ω_0.

accuracy. A change of only 0.005 Å in the value of r_0 corresponds to an increase of L greater than 25%. We can therefore conclude that the accuracy on the parameter r_0 is on the order of 0.001 Å. The fitting procedure also provides very useful information about the shape of the rotational potential of the H_2 ligand by way of the quantities V_0 and α. This type of detail could not have been obtained from *ab initio* calculations because they result from a very subtle modification in the coordination sphere, which is not taken into account by the relatively crude *ab initio* model.

As expected, the fourth parameter ω_0 is less accurately determined in our fitting procedure. The tunnel effect probed by the INS experiment involves only vibrational levels near the bottom of the well. For these energy levels the vibration (ω_0) along r is in its ground state and does not influence the tunnel effect to a great extent. Consequently the position of the levels and hence the observed transitions are less sensitive to this parameter. Our model is therefore not very suitable for extracting the H−H vibrational frequency from the low-frequency INS transitions, but it is a very accurate model for obtaining the H−H bond distance and shape parameters for the rotational potential.

Structural Parameters for Four Molecular Hydrogen Complexes

Four molecular hydrogen complexes with different types of ligands and metals have been chosen to test our model. While the electron count on the metal for all the complexes is formally d^6, the donating power of the ligands varies so that one would expect to find different values for the barrier to rotation of H_2 (V_0) as well as the equilibrium H−H bond distance (r_0). Strongly donating ligands increase the electron density on the metal and thereby enhance the back-donation to H_2, which leads to relatively long H−H distances (0.9 Å or above). But nothing can be said, *a priori*, about the influence of the donating power of the ligands on the value of the barrier to rotation. The four complexes we have selected illustrate the various situations that occur.

$IrClH_2(H_2)(P^iPr_3)_2$.[35] The complex $IrClH_2(H_2)(P^iPr_3)_2$, synthesized by Jensen et al.,[36] was the first neutral iridium molecular hydrogen complex. It has been extensively studied, and the binding energy of H_2 to the ML_5 fragment $IrH_2Cl(P^iPr_3)_2$ as well as the activation energy for this reaction are known from experiment.[37] The low reaction enthalpy of −6.8 kcal·mol^{-1} (the binding of H_2 is thermodynamically favored) shows that the H_2 ligand is not strongly bound to the metal, and one expects the rotation of H_2 to be easy. Indeed this compound was found to have the lowest barrier to rotation ever determined by INS for an H_2 complex, namely, 0.5 kcal·mol^{-1}.[35] *Ab initio* calculations on the same compound failed to reproduce this barrier to rotation with a calculated value of 2.2 kcal·mol^{-1}, which illustrates the difficulty of computing rotational barriers of H_2 in these complexes. Binding energies, on the other hand, are easier to compute accurately as indicated in a recent theoretical study which found the reaction enthalpy to be −7.2 kcal·mol^{-1}.[38]

Table 2. Calculated and Experimental INS Transition (cm^{-1}) for $IrH_2Cl(H_2)(P^iPr_3)_2$ and Parameters Obtained within the 1D and the 2D Models (V_0, in kcal·mol^{-1}; α, deg; r_0, Å; ω_0, cm^{-1})

	ω_t	ν_1	ν_2	ν_3	V_0	α	r_0	ω_0
exptl	19.9	127	221	270				
calcd[a]	19.9	132	219	270	0.69	69	0.782	3183
calcd[b]	19.9	135	211	272	0.46	141	0.78	

[a] 2D model. [b] 1D model.

In the previous 1D model used by Eckert to account for transitions observed by INS, the H−H bond distance has to be *assumed*. In this case where no structural information is available, the choice is difficult, and a value of 0.82 Å was chosen which corresponds to a typical distance in H_2 complexes. Lack of agreement between the 1D model and experiment can then be corrected by modification of the *fixed* H−H distance and/or by addition of a V_4 term in the potential $V(\phi)$ (eq 3).[23] In our 2D model both contributions (influence of r and of the V_4 term) are automatically included, and the resulting equilibrium H−H distance r_0 as well as the value for α are obtained *independently* from our fitting procedure.

The results obtained with both models are shown in Table 2 (see Figure 1 for definitions of ω_t and ν_i). The calculated transitions are in excellent agreement with the experimental ones, and the differences lie within the experimental error bars. The 2D model clearly improves the agreement over the 1D model where two transitions (ν_1 and ν_2) were reproduced with less accuracy. It should be noted that the H−H distance obtained in the fitting procedure of the 2D model is almost identical to the one assumed in the 1D model (see Table 2). This H−H bond distance is rather short (for a molecular hydrogen complex), and agrees with the experimental observations that the binding energy of H_2 is low and that the complex can readily lose H_2.[37,38] The frequency obtained for the H−H stretch (ω_0 in Table 2) is also indicative of a strong H−H interaction maintained within the H_2 ligand, although this value must be taken with caution as already stated.

Both the barrier to rotation obtained with the 2D model (0.69 vs 0.46 kcal·mol^{-1}) and the shape of the potential $V(\phi)$ differ appreciably from those derived by use of the 1D model. The parameters for the PES derived from the 1D model result in a global minimum at $\phi = 0$ and a higher (+0.46 kcal·mol^{-1}) local minimum at $\phi = 90$, while the 2D model does not require any secondary minimum in the PES. Moreover, an *ab initio* calculation on $IrClH_2(H_2)(PH_3)_2$ in a conformation corresponding to $\phi = 90$ has been optimized as a transition state.[39] The shape of the PES around $\phi = 0$ is also significantly different for the two models. The 1D model exhibits a steep well whereas the 2D model suggests a softer rotational motion from the

(35) Eckert, J.; Jensen, C. M.; Jones, G.; Clot, E.; Eisenstein, O. *J. Am. Chem. Soc.* **1993**, *115*, 11056.
(36) Mediati, M.; Tachibana, G. N.; Jensen, C. M. *Inorg. Chem.* **1990**, *29*, 3.
(37) Hauger, B. E.; Gusev, D. G.; Caulton, K. G. *J. Am. Chem. Soc.* **1994**, *116*, 208.
(38) Clot, E.; Eisenstein, O. *J. Phys. Chem. A* **1998**, *102*, 3592.
(39) Clot, E. Unpublished result.

Table 3. Calculated and Experimental INS Transition (cm^{-1}) for $Tp^{Me_2}RhH_2(H_2)$ and Parameters Obtained with the 2D Model (V_0, kcal·mol^{-1}; α, deg; r_0, Å, ω_0, cm^{-1})

	ω_t	ν_1	ν_2	ν_3	V_0	α	r_0	ω_0
exptl	6.7	126	194	203				
calcd	7.2	128	194	204	0.65	115.7	0.963	1619

equilibrium geometry (Figure 4). The picture provided by the 2D model is thus in better agreement with the general understanding of the M−(H_2) interaction. The small lengthening of the H−H distance at equilibrium is suggestive of weak back-donation from the metal, which is in better agreement with an easy rotation of H_2. The electronic origin of this weak back-donation has been previously discussed.[38]

$Tp^{Me_2}RhH_2(H_2)$ (Tp^{Me_2} = Hydrotris(3,5-dimethylpyrazolyl)borate).[19] Most of the H_2 complexes contain phosphine, cyclopentadienyl, or organometallic donors as coligands. These ligands are assumed to donate sufficient electron density to the metal to strengthen the M−(H_2) interaction. The complex $Tp^{Me_2}RhH_2(H_2)$ is the first example of a dihydrogen complex which contains only nitrogen donors as coligands. In Table 3 the results obtained with the 2D model are compared to the experimental results. In this case the agreement is also excellent. It should be noted that the model system $TpRh(H_2)H_2$ has been studied by DFT (B3LYP) calculations by Lledós and co-workers.[40] The optimized H−H distance was 0.836 Å, and the barrier to rotation of the H_2 ligand was 0.45 kcal·mol^{-1}. Tunneling calculations on a 1D potential derived from the *ab initio* results yielded a rotational tunneling ω_t of 9.2 cm^{-1}. This illustrates the difficulty to quantitatively describe INS experiments from *ab initio* calculations (see Table 3 for comparison).

The optimized parameters (Table 3) show an easy rotation (V_0 = 0.65 kcal·mol^{-1}) for such an elongated dihydrogen complex (r_0 = 0.963 Å). The H−H equilibrium bond distance extracted from the INS transitions is long, and suggests that the H_2 ligand is quite activated. This is supported by the fact that chemical substitution in the Tp^{Me_2} ligand leads to a drastic change in the structure of the complex: when one methyl (in Tp^{Me_2}) is substituted by a more electron withdrawing group like CF_3, the molecular H_2 complex is favored, while replacement of one H in Tp^{Me_2} by a methyl group to yield Tp^{Me_3} results in the formation of the dihydride.[41,42] The complex with Tp^{Me_2} is therefore at the borderline between the two domains.

While no diffraction structure is available for this compound, other experimental evidence such as a low value of the J(H,D) coupling constant favors a long H−H bond. The reported value of 4.7 Hz must be viewed as an average over all the possible isotopomers so that the true J(H,D) coupling constant for the H−D ligand would be 6 times greater if a purely statistical distribution of isotopomers is assumed. The resulting value of 28.2 Hz can be used with the correlation derived by Heinekey and co-workers[18] to obtain an H−H distance of 0.966 Å. Our computed value of 0.963 Å is thus in excellent agreement with the H−H distance estimated in this manner by NMR.

The experimental value of 2238 cm^{-1} for ν(HH)[19] is very low and also shows that the H−H interaction within the H_2 ligand is relatively weak. Our optimized parameter for ω_0 is also very low (1619 cm^{-1}; see Table 3) and indicative of the significant H−H bond activation. The apparent discrepancy between these two values is likely the result of the coupling of ν(HH) with the M−(H_2) stretch as was demonstrated for the Kubas compound.[27] Such a coupling is not included in our model and thus may account for the large difference in ν (HH) values.

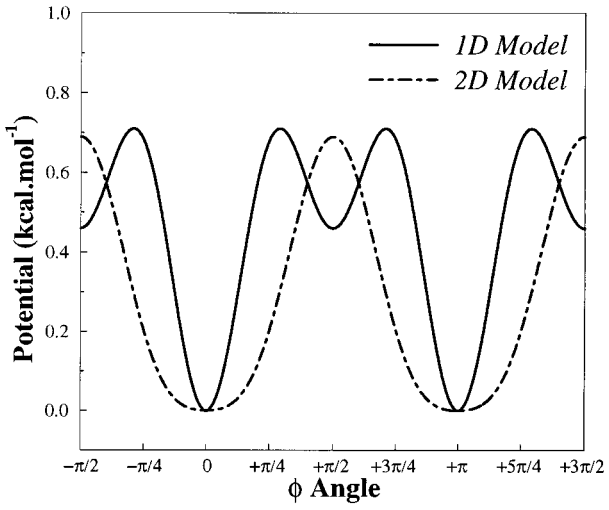

Figure 4. Comparison between the potentials $V(\phi)$ obtained with the 1D and 2D models for the compound $IrH_2(H_2)Cl(P^iPr_3)_2$.

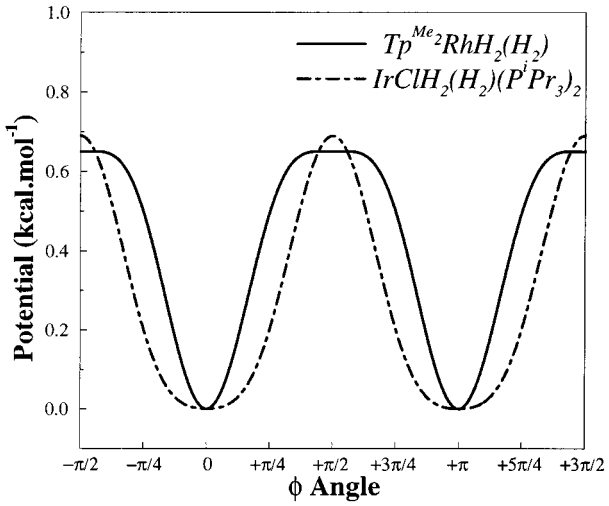

Figure 5. Comparison between the potentials $V(\phi)$ obtained for the compounds $IrH_2(H_2)Cl(P^iPr_3)_2$ (dashed line) and $Tp^{Me_2}RhH_2(H_2)$ (solid line) with the 2D model.

One of the interesting aspects of our results for this complex is the very low barrier to rotation obtained for such an elongated H_2 ligand. The observed barrier is practically the same as in $IrClH_2(H_2)(P^iPr_3)_2$, where r_0 was found to be just 0.78 Å. At first glance this seems paradoxical since we would associate a high degree of H−H bond activation with a strong M−(H_2) interaction, and would assume that the latter gives rise to a high barrier to rotation. A careful study of the shape of the V potential, however, shows that this may not always be the case.

In Figure 5 we compare the $V(\phi)$ potential for the two compounds. The principal difference arises from the respective values of α which result in two significantly different shapes for the rotational potential. As described above the potential for $IrClH_2(H_2)(P^iPr_3)_2$ (dashed line in Figure 5) suggests that the rotational motion about the equilibrium conformation (ϕ = 0) is easy because the back-donation is weak, while for $Tp^{Me_2}RhH_2(H_2)$ (solid line) the increase around ϕ=0 is much steeper, which implies a more difficult rotation for the H_2 ligand. This is in perfect agreement with the longer H−H distance found

(40) Gelabert, R.; Moreno, M.; Lluch, J. M.; Lledós, A. *Organometallics* **1997**, *16*, 3805.
(41) Bucher, U. E.; Lengweiler, D.; von Philipsborn, W.; Venanzi, M. L. *Angew. Chem., Int. Ed. Engl.* **1990**, *29*, 548.
(42) Bucher, U. E. Dissertation No. 10166, ETH Zurich, 1993.

Table 4. Calculated and Experimental INS Transition (cm^{-1}) for $FeH(H_2)(dppe)_2^+$ (Top Lines) and $FeH(H_2)PP_3^+$ (Bottom Lines) and Parameters Obtained with the 2D Model (V_0, kcal·mol^{-1}; α, deg; r_0, Å; ω_0, cm^{-1})

	ω_t	ν_1	ν_2	V_0	α	r_0	ω_0
exptl	2.1	225	255				
calcd	2.5	233	249	2.24	57.3	0.822	2706
exptl	1.15	259	276				
calcd	1.35	262	274	2.54	62.2	0.839	3160

for the rhodium compound in comparison with the iridium complex. It illustrates the strength of the 2D model in that it enables the *r* coordinate to play a role in the dynamical process. The very soft motion along *r* ($\omega_0 = 3183$ for Ir and $\omega_0 = 1619$ for Rh) makes it possible to reach configurations where H_2 can rotate more easily for the rhodium complex. This can be attributed to the very flat nature of the potential for a wide range of ϕ at the top of the PES.

$FeH(H_2)(dppe)_2^+$ and $FeH(H_2)PP_3^+$ Compounds.[43,44] A comparison of these two compounds is interesting since they differ mainly in the nature of the phosphine ligands and the cis versus trans arrangement of the hydride/H_2. Nonetheless, the INS spectra show rather different sets of transitions, which illustrates the sensitivity of this technique to the *precise* nature of these complexes. The experimental consequences of such differences in the ligand sets would be very difficult to reproduce by *ab initio* calculations because these generally model the phosphines by PH_3.

The two iron complexes are both cationic with four P atoms bound to the metal (dppe = $Ph_2PCH_2CH_2PPh_2$ and PP_3 = $P(CH_2CH_2PPh_2)_3$). Table 4 shows the results obtained for these complexes. Only two transitions to torsional excited states are observed experimentally, which could lead to an inaccurate determination of ω_0. We will therefore not discuss the ω_0 values for these cases. The agreement between experimental and computed INS transition frequencies is reasonable but not as good as for the two previous systems. The optimized fitting parameters contain several interesting points. When only strong donors such as H or P are present, the barrier to rotation is relatively high (above 2.0 kcal·mol^{-1}). The actual nature of the phosphine then simply modulates the overall value. From the V_0 values (2.24 kcal·mol^{-1} for dppe and 2.54 kcal·mol^{-1} for PP_3) one can infer that PP_3 is a stronger donating ligand than two dppe's. This conclusion is supported by the results for the other parameters which yield a wider potential (α = 62.2 vs α = 57.3) and longer H−H distance ($r_0 = 0.839$ vs $r_0 = 0.822$) for the complex with the PP_3 ligand.

A neutron diffraction structure of $FeH(H_2)(dppe)_2^+$ has been published,[7] and the experimental H−H distance of 0.82 Å is in excellent agreement with our computed value of $r_0 = 0.822$. Our model again reproduces the H−H equilibrium bond distance very well where it is known experimentally. The computed H−H distance obtained for $FeH(H_2)PP_3^+$ ($r_0 = 0.839$ Å) may thus be a very good estimate for the actual bond length. The higher value of the latter is also consistent with a higher electron density on the metal and hence the stronger back-donation. As described above this means that the rotation of H_2 in the PP_3 compound is initially more difficult than in the dppe compound, as indicated by the larger value of α, which makes the bottom of the well less shallow. However, this constitutes a small modification of the general picture, which is basically the same for the two systems. It does illustrate the power of INS for the characterization of very subtle effects which manifest themselves in the tunnel effect associated with the rotation.

Summary and Conclusion

We have developed a two-dimensional model to extract structural information from INS transitions for the dihydrogen ligand in metal complexes. This dynamical model explicitly includes the angle ϕ, which describes the rotation of the H_2 ligand, and the distance *r*, which corresponds to the internuclear separation between the hydrogen nuclei. These two coordinates are the ones most pertinent to the study of the rotational tunnel effect which arises from the easy permutation of the two identical nuclei.

The Schrödinger equation for a parametrized Hamiltonian is solved using a DVR representation for both coordinates with symmetry-adapted combinations for the ϕ coordinate. The reaction path Hamiltonian formalism coupled with the sequential adiabatic reduction was used to fully display the particular physics of the problem. The vibrational states corresponding to the large amplitude motion of the two hydrogen nuclei are obtained and the INS transitions computed.

A minimization of the least-squares fit of the differences between the calculated and observed transitions results in the *independent* determination of the four parameters introduced in the Hamiltonian. These parameters provide structural information about the M−(H_2) interaction and would be very difficult to obtain by ab initio methods. For the four systems studied the 2D model leads to a detailed analysis of the interactions between the metal and the H_2 ligand. Where experimental data are available, the results compare very well with the computed values. For example, the H−H distance in $FeH(H_2)(dppe)_2^+$ is 0.82 Å by neutron diffraction, and it is 0.822 Å with our model. This model offers a significant improvement over the 1D model which has previously been used. However, it is only useful if a sufficient number of INS transitions have been observed.

While instrumental limitations limit the observation of the tunneling transition by INS to those molecular hydrogen complexes with a barrier to H_2 rotation lower than approximately 3 kcal·mol^{-1}, transitions to the torsional states can in principle be observed for any such compound. Our methodology could be applied to such a case (albeit with somewhat lower precision) or, more generally, to any kind of experiment in which the dynamic process involves the permutation of two identical particles. For example, the quantum exchange coupling[45] phenomenon evident in the ^1H NMR spectra could be described by the same model Hamiltonian.[46] Or, if more data were available, one could describe the potential with more parameters (more terms in the $V(\phi)$ potential, anharmonicity in *r*), or add another coordinate that may be important (e.g., *z* or θ; see Figure 2). Our technical approach which built a very contracted and efficient zero-order basis would be highly appropriate for such extensions. We are currently working on this aspect.

Appendix

The Hamiltonian H of the dynamical model is the sum of the kinetic energy operator **T** (eq 1), which is a differential operator, and of the potential energy operator V (eq 10), which is a scalar operator. The ease of computation of the matrix elements of H with the basis functions depends on the choice made for their representation. Most often this representation

(43) Eckert, J.; Blank, H.; Bautista, M. T.; Morris, R. H. *Inorg. Chem.* **1990**, *29*, 747.
(44) Eckert, J.; Albinati, A.; White, R. P.; Bianchini, C.; Peruzzini, M. *Inorg. Chem.* **1992**, *31*, 4241.
(45) Sabo-Etienne, S.; Chaudret, B. *Chem. Rev.* **1998**, *98*, 2077.
(46) Kuhlman, R.; Clot, E.; Leforestier, C.; Streib, W. E.; Eisenstein, O.; Caulton, K. G. *J. Am. Chem. Soc.* **1997**, *119*, 10153.

consists of a set of orthonormal functions which allow computation of the matrix elements of **T** in analytical form. The basis set is usually a direct product of functions which are eigenfunctions of the various differential operators involved in **T**. In the variational basis representation (VBR),[32,47] the matrix elements of the potential operator are computed exactly, and this requires the most intensive computational effort. An alternative to this approach is the use of a discrete variable representation (DVR),[32] where the matrix elements of **T** are still easy to compute, but also those of V.

Since it is an approximate representation derived from the VBR, the DVR yields less accurate results. The matrix elements for the potential are evaluated by quadrature on grid points, and the size of the basis set (number of grid points) required to achieve a given accuracy is higher with the DVR than with the VBR. But the accuracy limitations apply mainly to the highly excited levels, while for the lowest vibrational levels the accuracy is comparable with the VBR results.[48,49] Moreover, some very efficient contraction schemes can be derived with the DVR. If a large amplitude motion is involved (rotation of H_2, for example), the sequential adiabatic reduction proposed by Bačić and Light[33,34] leads to a very accurate and efficient contracted basis set with which to solve the Schrödinger equation. In our case, the ϕ coordinate (Figure 2) is the slow variable while the r distance adapts itself to every change in ϕ. The sequential adiabatic reduction is thus applied by solving the Schrödinger equation for the variable r within a DVR for a fixed value ϕ_α for ϕ. Only the vibrational levels $E_n^{(\alpha)}$ under a given threshold E_o ($E_o = 25\,000$ cm^{-1} in our calculations) are kept, and then the Schrödinger equation for ϕ is solved on this basis of adiabatic states obtained for the different grid point values ϕ_α.[34]

The DVR is by construction isomorphic to another basis function representation called the finite basis representation (FBR).[32] In fact the DVR consists of a localization of the FBR basis functions on selected discrete points within a given range. The basis functions used to build the FBR are required to lead to an analytical expression for the matrix elements of **T**. For the ϕ coordinate, the kinetic energy operator is very simple (eq 1) and the FBR functions $|\varphi_k\rangle$ chosen are plane waves (eq 12).

$$\langle\phi|\varphi_k\rangle = (1/\sqrt{2\pi})e^{ik\phi} \qquad k = -2N - 1, ..., 2N + 1 \quad (12)$$

For the coordinate r, the kinetic energy operator can be written in a simpler form (eq 13). Because the model is a 2D model,

$$\mathbf{T}_r = -\frac{\hbar^2}{2\mu}\frac{\partial^2}{\partial r^2} \quad (13)$$

this rewriting leads to an extra potential term V_{ex} (eq 14) which has been added to the potential defined in eq 10. According to

$$V_{ex} = -\hbar^2/8\mu r^2 \quad (14)$$

the definition of $\mathbf{T_r}$ in eq 13, the sine functions have been chosen to build the FBR associated with the coordinate r (eq 15). The

$$\langle r|\psi_n\rangle = \sqrt{\frac{2}{a}}\sin\left[\frac{n\pi}{a}(r - r_{min})\right] \quad (15)$$

(47) Lill, J. V.; Parker, G. A.; Light, J. C. *J. Chem. Phys.* **1986**, *85*, 900.
(48) Hamilton, I. P.; Light, J. C. *J. Chem. Phys.* **1986**, *84*, 306.
(49) Bačić, Z.; Light, J. C. *J. Chem. Phys.* **1986**, *85*, 4594.

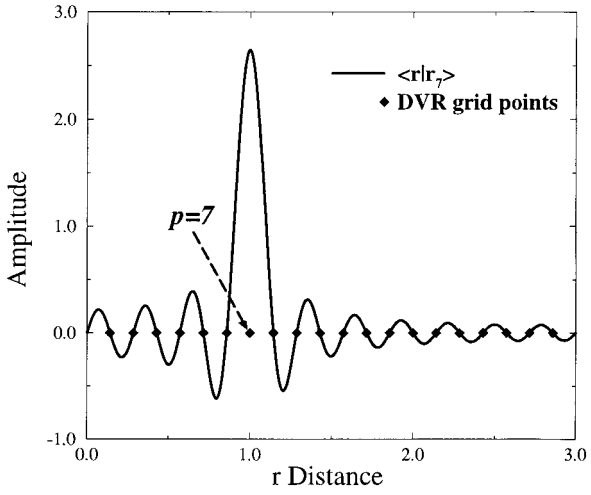

Figure 6. DVR function $|r_7\rangle$ corresponding to the parameters chosen for the calculations: $r_{min} = 0.0$ Å, $r_{max} = 3.0$ Å, and $M = 20$.

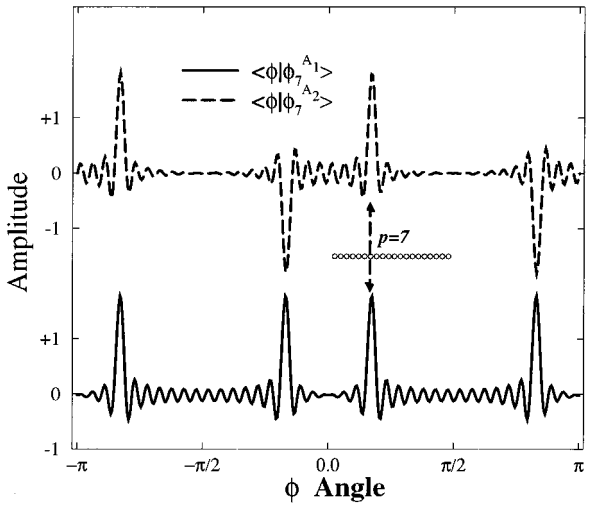

Figure 7. DVR functions $|\phi_7^{A_1}\rangle$ and $|\phi_7^{A_2}\rangle$ corresponding to the parameters chosen for the calculations: $\phi_{min} = -\pi$, $\phi_{max} = \pi$, and $N = 20$. The DVR grid points (open circles) are defined only within the range $[0, \pi/2]$, and the symmetry properties generate the function on the whole range.

range spanned by r during the rotation is assumed to lie between r_{min} and r_{max} ($a = r_{max} - r_{min}$), which is a good approximation for a rotating H_2 ligand ($r_{min} = 0.0$ Å and $r_{max} = 3.0$ Å). The DVR associated with this FBR consists of $M + 1$ points where $\langle r|\psi_{M+1}\rangle = 0$ (eq 16). The two extreme points r_{min} and r_{max} are

$$r_p = r_{min} + \frac{ap}{M+1} \qquad p = 1, ..., M \quad (16)$$

not included in the DVR, which is shown in eq 17. As a typical

$$|r_p\rangle = \sqrt{\frac{2}{M+1}}\sum_{n=1}^{M}\sin\left\{\frac{np\pi}{M+1}\right\}|\psi_n\rangle \quad (17)$$

example of the process of localization on going from a FBR to a DVR, $\langle r|r_7\rangle$ for $M = 20$ is shown in Figure 6. This function is zero on every grid point but r_7. This ensures the orthonormality of the DVR basis.

For the coordinate ϕ we have used the symmetry properties (Table 1) to build a symmetry-adapted DVR $|\phi_\alpha^{\Gamma_i}\rangle$.[50] The four irreducible representations lead to the following expression with ϕ ranging from $-\pi$ to π.

$$\langle\phi|\phi_\alpha^{A_1}\rangle = \sqrt{\frac{1}{(4N+2)\pi}} + \sum_{k=1}^{N}\sqrt{\frac{4}{(2N+1)\pi}}\cos\left[\frac{2k\alpha\pi}{2N+1}\right]\cos 2k\phi \qquad \alpha = 1, ..., N \quad (18)$$

$$\langle\phi|\phi_0^{A_1}\rangle = \sqrt{\frac{1}{(4N+2)\pi}} + \sum_{k=1}^{N}\sqrt{\frac{2}{(2N+1)\pi}}\cos 2k\phi \quad (19)$$

$$\langle\phi|\phi_\alpha^{B_2}\rangle = \sqrt{\frac{(-1)^\alpha}{(4N+2)\pi}} + \sum_{k=0}^{N-1}\sqrt{\frac{4}{(2N+1)\pi}}\cos\left[\frac{(2k+1)\alpha\pi}{2N+1}\right]\cos(2k+1)\phi \qquad \alpha = 1, ..., N \quad (20)$$

$$\langle\phi|\phi_0^{B_2}\rangle = \sqrt{\frac{1}{(4N+2)\pi}}\cos[(2N+1)\phi] + \sum_{k=0}^{N-1}\sqrt{\frac{4}{(2N+1)\pi}}\cos\left[\frac{(2k+1)\alpha\pi}{2N+1}\right]\cos(2k+1)\phi \quad (21)$$

(50) Leforestier, C. Private communication.

$$\langle\phi|\phi_\alpha^{B_1}\rangle = \sum_{k=1}^{N}\sqrt{\frac{4}{(2N+1)\pi}}\sin\left[\frac{(2k-1)\alpha\pi}{2N+1}\right]\sin(2k-1)\phi \qquad \alpha = 1, ..., N \quad (22)$$

$$\langle\phi|\phi_\alpha^{A_2}\rangle = \sum_{k=1}^{N}\sqrt{\frac{4}{(2N+1)\pi}}\sin\left[\frac{2k\alpha\pi}{2N+1}\right]\sin 2k\phi \qquad \alpha = 1, ..., N \quad (23)$$

In our calculations we have used $N = 35$ for the ϕ coordinate. Two examples of the symmetry-adapted DVR functions for ϕ are plotted In Figure 7. Only grid points between $\phi = 0$ and $\phi = \pi/2$ are needed for building the DVR, and the use of the symmetry properties generates a function defined over the whole range $[-\pi, \pi]$. Without imposing *a priori* symmetry, a DVR (and hence a FBR) 4 times greater would have been required. We have thus derived a very accurate and very efficient scheme to solve the Schrödinger equation for our parametrized model. Adjustments of the parameters were done by way of a least-squares fit to the experimental transitions. This implies solving the Schrödinger equation a large number of times, and the methodology we chose ensures the best compromise between accuracy and efficiency.

Acknowledgment. We thank Alberto Albinati, Claude Leforestier, and Odile Eisenstein for many helpful discussions and comments. Work at Los Alamos National Laboratory is supported by the Office of Science, U.S. Department of Energy. Los Alamos National Laboratory is operated by the University of California under Contract Number W-7045-ENG-36. This paper is dedicated to Odile Eisenstein and to the memory of her mother.

JA9836141